

DEPTH ESTIMATION FOR GEOTHERMAL RECONNAISSANCE DEDUCED FROM AEROMAGNETIC DATA OVER THE MAMBILLA PLATEAU AND ENVIRONS, TARABA STATE, NORTHEASTERN NIGERIA

*¹Yohana Andarawus, ²Othniel Kamfani Likkason, ³Maigari Abubakar Sadiq, ²Ali Sani, ¹Shekwonyadu Iyakwari, ⁴Adamu Abubakar, ⁵Mamidak Miner Iliya, ⁶Rawen Barnabas Ori and ⁷Ombugu Gideon

¹Department of Geology, Federal University of Lafia, Nigeria

²Department of Physics, Abubakar Tafawa Balewa University, Bauchi, Nigeria

³Department of Applied Geology, Abubakar Tafawa Balewa University, Bauchi, Nigeria

⁴Department of Applied Geophysics, Federal University, Birnin Kebbi, Nigeria

⁵Geology and Mining Department Nasarawa State University, Keffi, Nigeria

⁶Directorate of Remedial Studies, Abubakar Tafawa Balewa University, Bauchi, Nigeria

⁷Centre for Geodesy and Geodynamics, Toro, Bauchi, Nigeria

*Corresponding Author Email Address: yohana.andarawus@science.fulafia.edu.ng

ABSTRACT

The geothermal gradient, heat flow and Curie point depth (CPD) were calculated using aeromagnetic data to assess their viability in terms of energy generation around Mambilla plateau and environ, Northeast, Nigeria. Each block of spectral plot was used to determine the depths to the top boundary (Z_t), to bottom (Z_b) and centroid (Z_c). Empirical formula was used to calculate the geothermal gradient, Curie Point Depth (CPD) and heat flow in the area. The resulting depth measurements were then consider as the area's geothermal gradient, heat flow, and curie point depths (CPD). Two CPD locations with geothermal potential are described in the results: areas with shallow curie point depths (0.11-1.72 km) and areas with deeper curie point depths (0.34-4.46 km). The geothermal gradients measured range from 46.22 to 121.620°Ckm⁻¹, while the measured heat-flow values range from 139.16 to 304.05 mWm⁻². This study also reveals how complex magmatic and tectonic linkages of large intrusions and fault systems, particularly the Chain faults that may have extended into the study area, are related to geothermal systems. A common CPD of 3°C100m⁻¹ or 30°Ckm⁻¹ and average thermal conductivity values ranging from 105.68 to 227.63mWm⁻² are considered to have a good potential for geothermal energy. This result have strong and positive correlation with what is obtained in some countries were geothermal energy is been utilized for power generation. The potential for geothermal energy resources in the area is therefore very high. The study's most important and practical finding is that the area has good potentials for geothermal energy resources, which could be used to compliment the Government-owned Mambilla Hydro-Electric Power Plant, as a reliable renewable energy source.

Keywords: Geothermal, Curie Point Depth, Aeromagnetic, Isotherm and Mambilla

INTRODUCTION

Precambrian Basement Complex in Nigeria should have a heat flow of roughly 41-10 mW/m², which is the global average for continental Precambrian shields. However, there hasn't been much research done in Nigeria on that subject. Verheijen and Ajakaiye

(1979) conducted the only generally known heat flow estimation in the middle of the Ririwai ring complex, one of the granitic ring complexes of the Younger Granites Province of Northern Nigeria, situated beneath Precambrian shield. The average heat flow in the study's findings was 0.920.04 HFU (38.51.7 mW/m²), which is about the same as the global average.

The worldwide need for energy is rising to the point of a severe crisis, especially in developing nations, in response to the rising trends in the world's population, urbanization and industrialization. It is projected that the conventional sources of energy generation (thermal and hydro power plants) are finite and would not last very long if used at the current pace of use. Even though thermal and hydroelectric power plants account for more than 66.7% and 33.3% of the country's total electricity production, respectively, almost all of it is domestically produced, Nigeria still has a severe energy crisis because of its high reliance on imports for the necessary crude oil and other petroleum products as well as seasonal variations in water volume. Nigeria's inability to increase its electricity-generating capacity through hydro, nuclear, or other sources over the past decades has exacerbated the issue and led to frequent rolling blackouts due to electricity shortages throughout the nation, which in turn increased the unemployment rate of the nation. Due to weak government policy, bad administration, and an excessive reliance on natural gas and water as energy sources, Nigeria is predicted to have an increased energy crisis in the near future (Kurowska and Schoeneich, 2010). According to EIA (2007), just 40% of Nigeria's 200 million people have access to electricity, which is typically more readily available in urban, developed areas than in rural outlying areas.

Public and corporate sectors are constantly working to utilize the efficient renewable energy-generation sources, including hydel, solar, wind, and biomass. The geothermal energy sources, which comprise thermal or electrical power generated from the heat in the Earth, should also be given proper consideration in addition to these renewable energy sources because they have not previously been given top priority. Although Nigeria contains many surface manifestations of hydro-geothermal energy sources, none of the locations have yet been developed for the direct use of the thermal energy or for the generation of electricity (Kurowska and

Schoeneich, 2010). The majority of the readily accessible hydro-geothermal systems, such as those connected to hot springs, geysers, and fumaroles near the surface, are already well-known, and many have been created in a number of other nations. According to Dickson and Fanelh (2004) and Shibaki and Beck (2003), there were more than 25 countries with approximately 9000MW of installed geothermal electrical generation capacity as of 2003, with the majority of these being the United States, Philippines, Mexico, Indonesia, Italy, Japan, New Zealand, Iceland, Costa Rica, El Salvador, and Kenya. This amounts to about 0.25% of the total installed electrical generation capacity worldwide.

In actuality, the utilisation of hydro-geothermal energy only accounts for a small portion of geothermal energy's entire potential, which is mostly connected with the deeply buried hot dry rocks (HDRs), which are often found at depths of 4-6 km. The geothermal energy potential in the top 10 km of the Earth's crust has been calculated to be 50,000 times as powerful as all of the world's known oil and gas reserves (USD, 2002). Prior to current research and development efforts for the exploration of deep HDR sources and the cost-effective development of HDR geothermal energy exploitation technologies, i.e., enhanced geothermal systems (EGS), in nations like Australia, Germany, U.S.A. and Japan, these resources were not generally thought to be technologically or economically accessible (GEA, 2001). However, this is no longer the case.

The current work uses spectrum analysis of aeromagnetic data to characterise the Curie Point Depth, Geothermal gradient, and heat flow inside the Mambilla plateau and Environs, Northeastern Nigeria, as well as the depths to the top and bottom of the magnetised crust. Results will be helpful to Nigerian electricity producing businesses, especially now that potential alternative power sources are being investigated.

MATERIALS AND METHODS

Study Area Location, and its Geological Settings

The research area is situated in Sardauna and Gashaka Local Government Areas of Taraba State, Northeastern Nigeria. It is located between latitudes 6°30'00" and 7°30'00"N and longitudes 11°00'00" and 11°30'00"E, making up the southernmost tip of the eastern portion of Nigeria's northern region. According to Tukur et al. (2005), its entire land area is 6,050 km² (Fig. 1). This plateau is locked with Cameroon in the south, east, and west (Frantz, 1981). According to Mubi and Tukur (2005), the Basement Complex rocks, which date from the Precambrian to the early Paleozoic epoch, cover more than two thirds of the plateau. The remainder of the plateau and its surroundings are made up of volcanic rocks from the upper Cenozoic through Tertiary and Quaternary periods (Jeje, 1983). Trachyte and olivine basalt are among the volcanic rocks that make up the basaltic suite. Nigeria is in charge of the plateau's western slope and the remaining section of its northern escarpment, while the plateau's eastern and southern escarpments are situated along the Cameroon border (Mould, 1960; Dupreez and Barber, 1995). Precambrian basement complex and Phanerozoic rocks combine to form Nigeria's crystalline rocks. Throughout the geological history, these crystalline basement rocks have experienced deformation of varying intensities. As a result, significant fractures have appeared (Figure 1). As a result, Obaje (2009) identified NS, NE-SW, NW-SE, NNE-SSW, NNW-SSE, and to a lesser extent, E-W fractures.

One of the three main litho-petrological elements that make up Nigeria's geology is the Basement Complex (figure 1). The Pan-

African mobile belt includes the Nigerian basement complex, which is located south of the Tuareg Shield and between the West African and Congo Cratons. The Mesozoic calc-alkaline ring complexes (newer Granites) of the Jos Plateau intrude it, while Cretaceous and newer sediments are unevenly overlaid on top of it. The 600 Ma Pan-African orogeny had an impact on the Nigerian basement, which is located in the reactivated zone created by plate collision between the West African craton's passive continental margin and the active Pharusian continental margin (Burke and Dewey, 1972; Dada, 2006). According to Obaje (2009), the basement rocks are thought to be the product of at least four main orogenic cycles, including the Liberian (2,700 Ma), Eburnean (2,000 Ma), Kibaran (1,100 Ma), and Pan-African cycles (600 Ma). Additionally, Abaa and Najime (2006) investigated the locations of a number of ore minerals, including wolframite, galena, chalcopyrite, barite, and gem minerals, in the Oban-Obudu-Mandara-Gwoza region, which is located in the eastern portion of the Nigerian Basement complex.

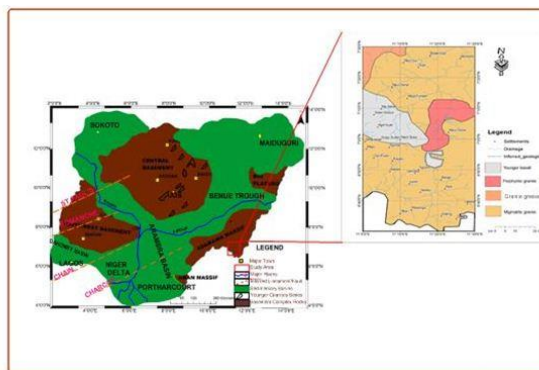


Figure 1: Geological map of the study area showing rock distributions and the prominent fracture zones in Nigeria (Modified after Udensi *et al.*, 2003)

About 48% of the country's total land area contains the Nigerian Precambrian basement complex, and the remaining 52% is covered by Cretaceous to recent sediments deposited in several basins (Fig. 1). In the western part of Nigeria, schists (metasediments) with quartzites and other minor lithologies are forming long, narrow, north-south trending belts. The basement complex of the central shield, south-western part, south-eastern, and eastern margin of the country is composed of three major groups of rocks: (1) migmatite and gneiss dominated (Liberian to Pan-African age), (2) intrusive granitic rocks

The largest and deepest sedimentary zone, which is mostly composed of various clastics of both marine and continental origin, is approximately 1 200 km long and trends from the Niger Delta in the southwest to the Benue Trough and towards the northeast to the Borno (Chad) Basin. This belt, which has multiple sub-basins, as well as its branches, are connected to the lower Cretaceous Gondwana breakup and the stretching and opening of the crust of the Atlantic Ocean (Gulf of Guinea). The basins, which have been largely interpreted as troughs and rifts, were impacted by magmatic volcanic eruptions and synsedimentary tectonic deformations between the Cretaceous and Neogene periods, resulting in the current structural pattern. This significant Nigerian sedimentary zone is deepest in the Niger Delta, where the maximum sediment thickness surpasses 9 km (Mattick, 1982). The Benue Trough is divided into three sections: the Lower Benue Trough, which

includes the Anambra Basin and the Abakaliki Anticlinorium (Uplift), and the Middle and Upper Benue Troughs, which include the Yola Arm, Gongola, and Kerri basins. In some areas of the trough, the maximum sediment thickness reaches even 6 km. The Borno Basin, a portion of the Nigerian Chad Basin that is 4 km thick with Cretaceous to Quaternary sediments, is overlaid by the Benue Trough in the north-east. Other authors have suggested that it may be even deeper than that, at 7 km deep (Ostaficzuk, 1996).

The Middle Niger Basin, also known as Nupe or Bida Basin, is a sizable western branch of the Benue Trough. It is just 0.5 to 1 km deep in most places and doesn't go over 2 km deep in the deepest regions (Ojo et al., 1989). In addition to the two primary provinces of rocks in Nigeria, which are Precambrian crystalline and Cretaceous to Quaternary sedimentary, there are also Cainozoic volcanic rocks, which are mostly found in the country's east. Many trachyte-phonolitic and basaltic plugs within Benue Trough and basaltic lava plateaus, of which the most notable are: Biu Plateau with its over 80 volcanoes and extensive basaltic lava flows of Jos Plateau, are the byproducts of Cainozoic magmatic and volcanic activity (Grant et al., 1972; Turner, 1978).

Additionally, specifically for Nigeria, the geological structure of the area affects the breadth of geothermal exploration inside each of the nation's geological provinces. Geothermal heat is distributed generally throughout the upper earth crust. Because those regions do not have any petroleum potential, drilling exploration and measurements of the subsurface temperature are not conducted there, hence nothing is known about the geothermal properties of basement rocks. Nigerian sedimentary basins have been investigated for hydrocarbons for a number of years, which explains the oil company's extensive collection of subsurface temperature data. Water boreholes, in addition to oil and gas exploration wells, are a reliable source of data on subsurface temperatures. The temperature recorded during pumping experiments is fairly close to the actual temperature of the rock formation that contains water. But these wells are typically small; because the water aquifers are typically located within soft overburden resting on top of hard crystalline rock mass, water wells drilled in crystalline locations in Nigeria typically are not deeper than 20-30 meters. Water boreholes can often be found in sedimentary regions 500 meters or deeper, and many of them can be used as a source of geothermal information. The surface manifestation of geothermal activity serves as the other geothermal data source. In Nigeria, there are a number of warm and hot springs and seepages that highlight the locations of possible geothermal anomalies, with the majority of them situated inside the Benue Trough's sedimentary basin.

Geothermal Investigation of Crystalline Province in Nigeria

Verheijen and Ajakaiye (1979) conducted the only generally known heat flow estimation in the middle of the Ririwai ring complex, one of the granitic ring complexes of the Younger Granites Province of

Northern Nigeria, situated beneath Precambrian shield. The average heat flow in the study's findings was 0.920.04 HFU (38.51.7 mW/m²), which is about the same as the global average. A thermal spring known as Ikogosi is situated inside the quartzite-schist formation of the Nigerian basement complex in the country's southwest. The spring water is 37 C in temperature. It serves as a swimming pool and is a popular local attraction. It is also likely the only location in Nigeria where geothermal energy is employed directly.

To the northwest of the Jos Plateau (central shield), in Rafin Reewa, close to Lere, a new warm spring has just been found. Spring water runs from migmatic and gneissic rock formations and is 42°C in temperature. The Jos Plateau is home to a number of springs, all of which serve the local populace with cool, pure water. Ikogosi Warm Spring's presence and certain recent discoveries imply that local anomalies can cause the distribution of geothermal heat within Nigeria's Precambrian basement rocks to vary (Kurowska and Schoeneich, 2010).

Volcanic and Geothermal Surface Manifestations in some African Countries

To describe the geothermal systems, all surface information about geothermal activity was gathered. All geothermal manifestations, such as volcanoes, hot springs, and geysers, are included in these data. AitOuali et al. 2019, Waring 1983, and Saibi et al. 2006 are only a few of the sources that were used to compile the locations of the hot springs throughout Africa, which were then combined in the GIS model. The fourth TL of evidence in the GIS model was these outward manifestations. Indicators of a subterranean heat source include volcanic features including craters, calderas, and active or young volcanoes. Due to their tectonic stability, the south and north of Africa have not yet been thought of as viable locations for the production of geothermal energy (Dhansay et al. 2014; Enerdata 2013); however, several Egypt, north Algeria, and South Africa are only a few examples of northern and southern African nations that feature surface thermal manifestations like hot springs with varying temperatures.

The Infrastructure Consortium for Africa and the United Nations Environment Programme estimate that Eastern Africa has a geothermal potential capacity of more than 20 GW of geothermal energy (Teklemariam 2018), which has encouraged nations like Comoros, Eritrea, Djibouti, Rwanda, Uganda, and Tanzania to start looking into geothermal resources. By 2021, Ethiopia has a goal of producing 1 GW of geothermal energy. In addition, new small-scale geothermal power facilities are being built in Zambia, Burundi, and Uganda (Hafner et al. 2018). Table 1 compiles the geothermal activities, temperature gradients, and heat flows of various African nations.

Table 1: Geothermal activities, temperature gradients, and heat flows of some African countries based on various previous works

Country	Geothermal activities	Geothermal gradient (°C/km)	Heat flow (mW)	References
Algeria	DU		100-120	(Meliani et al., 2016)
Botswana	DU, F		60-90	Leseane et al., 2015)
Burundi	DU, ES, EAR	> 60	72	(Sinziinkayo et al., 2015)
Cameroon		Avg of 72.24	Avg of 180.59	Mono et al., 2018)
Congo		40	30-40	(Schito et al., 2016)

Djibouti	IU, DU, EAR, ES		~ 235	(Saleh et al., 2013)
Egypt	DU	16.3–67.4	47.1–195.5	(Abdel Zaher et al., 2018; Elbarbary et al., 2018)
Ethiopia	IU, DU, EAR, ES, PP	60		(Bekele, 2012)
Gabon		Avg 33		(Hodgson et al., 2017)
Ghana			42 ± 8	(Sass & Behrendt, 1980)
Nigeria		46.22-121.62	105.68 - 227.63	Verheijen and Ajakaiye 1979, Yohanna et al, 2023

Aeromagnetic Data

The Nigerian Geological Survey Agency (NGSA) was where investigators bought the aeromagnetic data sheet used in this investigation. Sheets 276 and 295 are respectively composed by it. Fugro Airborne Survey Limited acquired the data sets for the NGSA in the years 2003–2009, DGRF–2005 deleted, and each on a scale of 1: 100,000 NGSA, (2008). The real-time differential GPS was used to carry out the survey in drape mode with a sensor mean terrain clearance of 75 meters. The flight and tie lines are oriented in NW-SE (SE) and NE-SW, respectively, according to NGSA, (2008). The spacings between the traverse and tie lines are 500 and 2,000 m. In accordance with Patterson (1985), Oladunjoye et al. (2016), the data sets were de-cultured, levelled, corrected for the International Geomagnetic Reference Field, and gridded at an appropriate cell size that enhances the information contained in the anomaly and suppresses the latitudinal influence and undesirable signal (noise). To export the field data to Oasis Montaj 8.4.2, the total magnetic intensity [TMI] was created in the x, y, and z formats (where x, y, and z denote longitude, latitude, and TMI, respectively). In order to compare the resulting maps with the geological map of the research area, the Universal Transverse Mercator values for x and y were converted to geographic coordinates using the Rockware TM 15 software. The residual magnetic intensity (RMI), which was created by eliminating the regional magnetic field strength from the data, was used to improve the local subsurface features. Because the research location is in the low magnetic latitude zone, the reduction-to-equator (RTE) filter on Geosoft Oasis Montaj was employed to improve the features on TMI data. According to Okpoli (2019), RTE removes the magnetic latitudinal influences, centers the peaks of magnetic anomalies on their sources, and makes the Earth's magnetic field and magnetization of the magnetic sources look horizontal. Using the two-dimensional fast Fourier transform (2D-FFT) method, the RTE was carried out. The mean values for inclination and declination were 11.10 and 4.90, respectively. According to Oladunjoye et al. (2016), the complicated information that is embedded in the original data is made simpler by using 2D-FFT on potential field data. Additionally, it raises the standard of data being processed for accurate geological inferences. One of these simplifications involves creating maps where the displayed function's amplitude is either directly or indirectly related to a rock's physical characteristic as well as to its natural structural characteristics and other required criteria. Using the Geosoft Oasis Montaj workstation, the RTE-RMI data were additionally subjected to depth continuation (upward continue) enhancement techniques as used by (Awoyemi et al, Awoyemi et al 2016, Awoyemi et al 2017, Awoyemi et al 2018, Oladunjoye et al, 2016, Okpoli, 2019, Anudu et al 2014, Ogunmola et al, 2016, Olasunkanmi et al, 2017, Olasunkanmi et al, 2018) . We used the spectrum analysis method to estimate the CPD using the obtained aeromagnetic data. The magnetic layer is thought to be infinitely long in all horizontal directions by Tanaka et al. (1999). Since the horizontal scale of the magnetic source is significantly

larger than the depth to the top of the magnetic source, the magnetization of the layer $M(x, y)$ is a random function of x and y .

Estimating Depth to Magnetic Sources

In order to calculate the depth to the base for a single window, Okubo et al. (1985) devised an algorithm to estimate the basal depth from magnetic data. The technique then uses the slope of the magnetic anomalies radially averaged power spectrum to determine the depth to the centroid (Z_0) and to the top (Z_t) of the magnetic source. The power-density spectra of the total field anomaly were given by Blakely (1995) as follows: $\Phi_{\Delta T}$:

$$\Phi_{\Delta T}(K_x, K_y) = \Phi_M(K_x, K_y) \times F(K_x, K_y), \quad 1$$

$$F(K_x, K_y) = 4\pi^2 c_m^2 |\Theta_m|^2 |\Theta_f|^2 e^{-2|k|Z_t} (1 - e^{-|k|(Z_b - Z_t)})^2 \quad 2$$

Φ_M is power-density spectra of the magnetization, C_m is a proportionality constant, Θ_m and Θ_f are factors for magnetization direction and geomagnetic field direction, and Z_a and Z_b are top and basal depth of magnetic source, respectively.

The above equation can be simplified by noting that all terms, except $|\Theta_m|^2$ and $|\Theta_f|^2$ are radially symmetric. Moreover, the radial average of Θ_m and Θ_f are constant. If $M(x, y)$ is completely random and uncorrelated, $\Phi_M(K_x, K_y)$ is a constant. Hence, the radial average of $\Phi_{\Delta T}$ is:

$$\Phi_{\Delta T}(|K|) = A e^{-2|k|Z_t} (1 - e^{-|k|(Z_b - Z_t)})^2 \quad 3$$

where A is a constant and k is a wavenumber. For wavelengths less than about twice the thickness of the layer, Eq. (3) can be simplified

$$\ln[\Phi_{\Delta T}(|K|)^{1/2}] = \ln B - |k|Z_t, \quad 4$$

where B is a constant. Eq. (3) can be rewritten as:

$$\Phi_{\Delta T}(|K|)^{1/2} = C e^{-|k|Z_0} (e^{-|k|(Z_t - Z_0)} - e^{-|k|(Z_b - Z_0)}), \quad 5$$

where C is a constant. At long wavelength, Eq. (5) can be written as:

$$\Phi_{\Delta T}(|K|)^{1/2} = C e^{-|k|Z_0} (e^{-|k|(-d)} - e^{-|k|(d)}) = C e^{-|k|Z_0} 2|k|d \quad 6$$

where $2d$ is the thickness of the magnetic source. Eq. (6) can be presented in another form as:

$$\ln\{\Phi_{\Delta T}(|K|)^{1/2}/|k|\} = \ln D - |k|Z_0 \quad 7$$

where d is a constant. By fitting a straight line through the high and low wave number parts from the radially average power spectrum

of $\ln[\Phi_{\Delta T}(1Kl)^{1/2}]$, $\ln\{\Phi_{\Delta T}(1Kl)^{1/2}/|k_l|\}$, Z_t and Z_0 can be estimated. Finally, the basal depth of the magnetic source (Okubo et al., 1985; Tanaka et al., 1999) is:

$$Z_b = 2Z_0 - Z_t \quad 8$$

The geothermal gradient (dT/dz) between the Earth's surface and the CPD (Z_b) can be defined by Eq. (9) (Tanaka et al., 1999; Stampolidis et al., 2005; Maden, 2010):

$$\frac{dT}{dz} = \frac{580^\circ\text{C}}{Z_b} \quad 9$$

In addition, the geothermal gradient can be associated to the heat flow q by using Eq. (10) (Turcotte and Schubert, 1982; Tanaka et al., 1999) and assuming no radioactive source:

$$q = \lambda \left(\frac{dT}{dz} \right) = \lambda \left(\frac{580^\circ\text{C}}{Z_b} \right) \quad 10$$

where λ is the coefficient of thermal conductivity.

Data windowing was used to calculate the radial power spectrum in order to estimate the CPD from a 2D magnetic map. The depth resolution in such calculations is constrained to the width of the aeromagnetic window (L), whereby the maximum CPD depth estimation is limited to $L/2\pi$ (Shuey et al., 1977). In each window, both power spectrum and scaled-frequency power spectrum were calculated in order to calculate the depth to top (Z_t) and centroid (Z_0) depths of magnetic sources. From the relation of $Z_b = 2Z_0 - Z_t$, the curie depth point (Z_b) was computed, following the Okubo et al. (1985) procedure.

RESULTS AND DISCUSSION

Total Magnetic Anomaly Intensity Reduced to the Equator (RTE)

A combination of regional, residual, and noise signals can be seen on the total magnetic intensity map. The shallow magnetic sources connected to intrusive bodies like dykes and plutons are responsible for the short-wavelength components. The presence of outcrops of gneiss-migmatite complex or the presence of rocks at shallow depths may be the cause of the high magnitude of the strong amplitude magnetic anomaly. The research area's high magnetite concentration regions and the high magnetic anomalies could both be related to the northwestern Nigerian migmatite-gneiss complex. Values are displayed on the total magnetic intensity map, ranging from 32892.772 nT to 33203.596 nT. According to Sunday (2012), the TMI map that was produced includes high, low, and intermediate magnetic signs that can be attributed to the rock's susceptibility, its depth from the source of the magnetic rock, its degree of strike, and its residual magnetization. The communities Gidan Garba, Maisamari, Gidan Godiya, Nguroje, Ngubio, Banga, Kaker, and Kilating had the highest TMI values (Figure 2). The communities of Mayo Juji, Bode Goje, Ida Manti, Mayo Selbe, Mayo Fundam, and Kara (Figure 3) likewise had intermediate levels. The villages of MajoTolore, NgelNyeki, Kuuku, Dan Fulani, Magu, and GidanGodiya, respectively, had the lowest values. The primary data of qualitative analysis is trends and lineation, which are typically an indicator of the characteristics that give rise to faults and fractures (Udensie et al., 2003). The Northeast-Southwest trends are the dominant trend and lineation in the study area (Fig. 2), and they can be seen in the

following locations: Majo Tolore, NgelNyeki, Kuuku, Dan Fulani, Magu, Gidan Godiya, Mayo Juji, Bode Goje, Ida Manti, Mayo Selbe, Mayo Fundam, and Kara. The shallow magnetic sources connected to intrusive bodies like dykes and plutons are responsible for the short-wavelength components. The gneiss-migmatite complex outcrops or the rocks existing at shallow depths in the research area may be the cause of the high magnitude of the strong amplitude magnetic anomaly. The study area may be connected to the migmatite-gneiss complex in northeastern Nigeria because the strong magnetic anomalies correspond to areas with significant magnetite content.

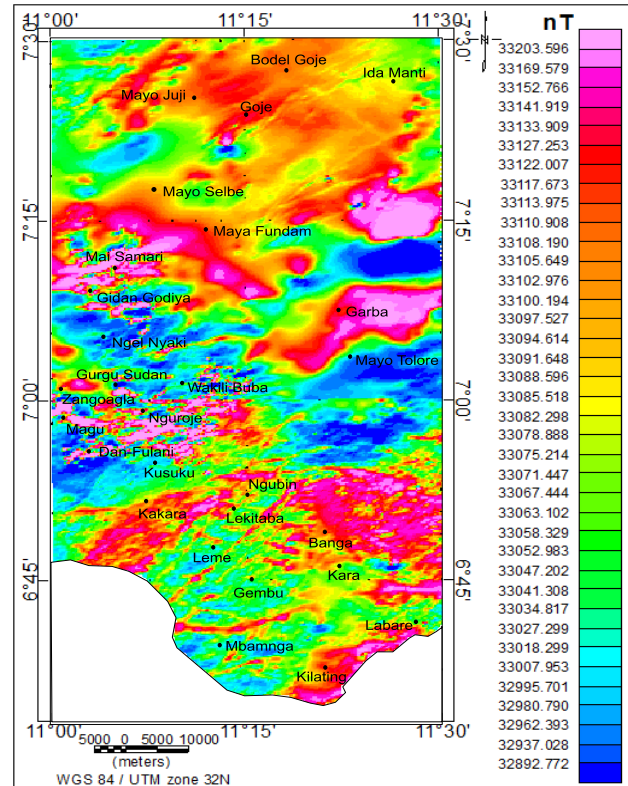


Figure 2: Total magnetic intensity map of Mambilla and environs

The Main Magnetic field map over Mambilla and environs

The average value of the main magnetic field over Mambilla and its surroundings is 33228.522 nT to 33358.377 nT (Figure 3). Using the total magnetic intensity map of the research area (TMI), this field represents the regional field of the study area that has been subtracted from the residual or crustal field of the area. The communities of Kilating, Kara, Leme, Dan Fulani, Mbanga, and Gembu, which trend NW-SE (Figure 3) and gradually grow from SW-NE, had the lowest main fields. From Ida Marti to Bode Goje, the main field similarly grows, with the highest main field being found in the study area's far northeast. The major field's overall pattern is NW-SE (Figure 3).

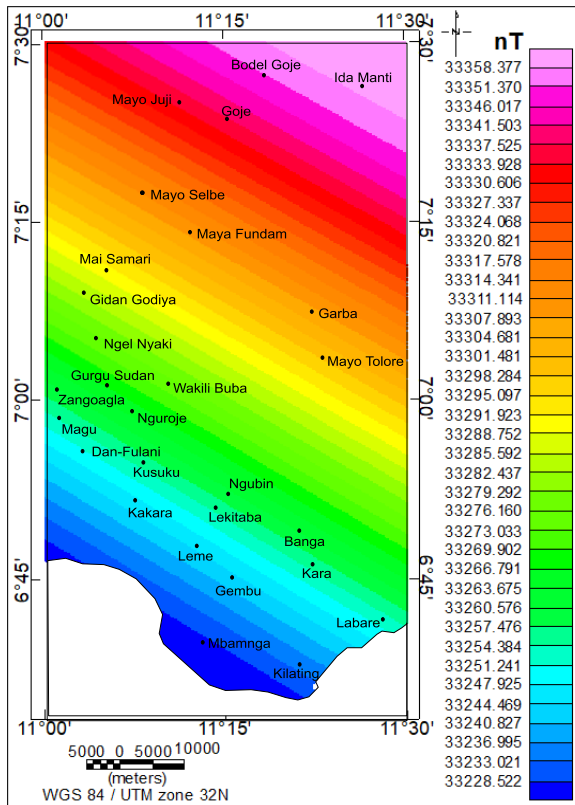


Figure 3: The main magnetic field map of Mambilla and

The crustal magnetic field map of Mambilla and environs

An average value of -159.50nT is shown on the crustal magnetic field map over Mambilla and its surroundings, with values ranging from -397.669nT to -80.699nT. This area is affected by localised or causative bodies. An indicator that there are variations in the geological, magnetic, and chemical compositions of the rock's bodies is the fluctuation in the crustal magnetic field within the studied area.

The varying crustal magnetic field within the studied area is a sign that the rock's bodies have different geological, magnetic, and chemical compositions. The values displayed by the map of the study area's crustal field are all negatives, indicating that the region is a magnetic equatorial region (Figure 4).

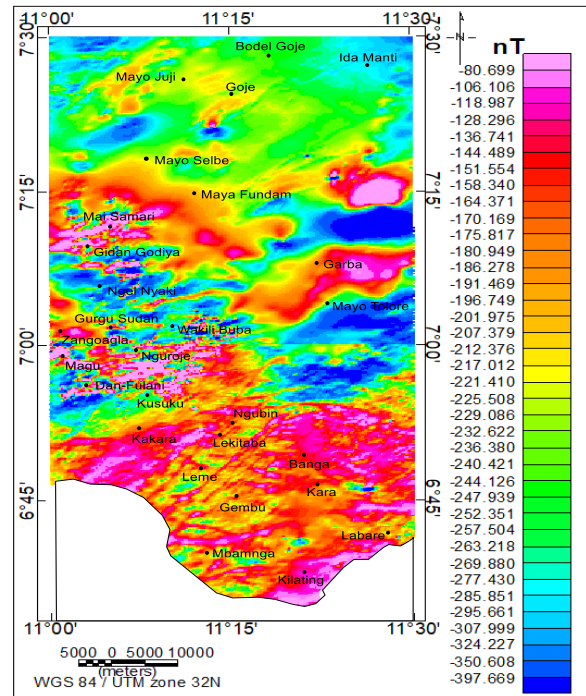


Figure 4: The crustal magnetic field map of Mambilla

Reduction to the Equator Map of Mambilla and Environs (RTE)

This operation transforms the observed TMI into the anomaly that would have been measured if the magnetization and ambient field were both horizontal. It is therefore possible to have magnetic anomalies over their causative source facilitating the interpretation of geological features (Noutchogwe et al., 2010). The reduction to the equator (RTE) procedure was used to maintain the equator's low angle of inclination, which made the source of magnetization horizontal (Fig. 6). Due to the study area's low angle of inclination, the RTE's output resembles the magnetic anomaly map of that region. The RTE map enhances the basement architecture, including structural lineaments with its orientations, and helps to remove the magnetic inclination impact in the low magnetic latitude zone by centering the peaks magnetic anomalies over their sources. On the basis of the variance in magnetic intensity across the study area, two significant magnetic zones were identified. High amplitude magnetic anomalies are most prevalent in the western, central, southern, and eastern regions (between -82.382nT and -119.153nT). However, the area's extreme northern and northern-western regions are distinguished by relative low amplitude magnetic intensity values (between -130.00nT and -392.122nT) marked with greenish to blue colours, indicating regions with low magnetic content in geological structures (fault/fracture).

The RTE map enhances the basement architecture, including structural lineaments with its orientations, and helps to remove the magnetic inclination impact in the low magnetic latitude zone by centering the peaks magnetic anomalies over their sources. On the basis of the variance in magnetic intensity across the study area, two significant magnetic zones were identified. High amplitude magnetic anomaly values are dominant in the western, central, southern, and eastern portions. However, relative low amplitude magnetic intensity values are seen in the area's extreme northern, western, and southern regions (Figure 5). According to Ngako et al. (2008), the RTE map primarily features northeast-trending

minima and maxima anomalies that are broadly parallel to the strike-slip tectonic episodes connected to Proterozoic collisional events.

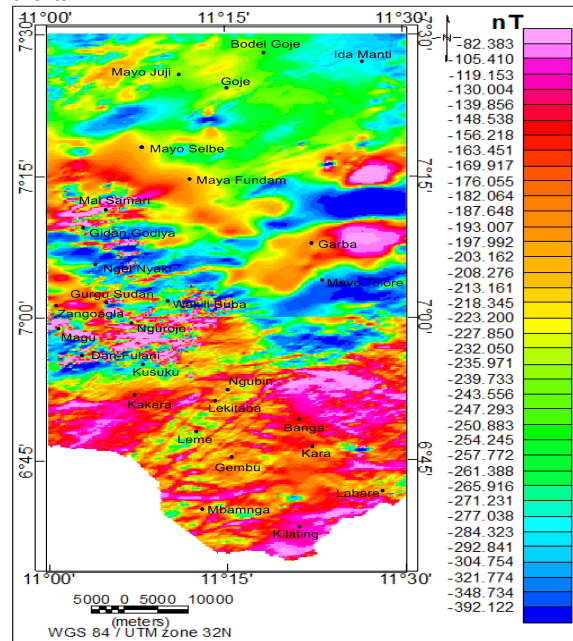


Figure 5: The Reduction Magnetic Equator map of Mambilla and Upward Continued Crustal Magnetic field Map of Mambilla and Environs

The magnetic equator field map reduction over Mambilla and its surroundings was continued northward for another 15 km, showing values ranging from -279.141nT to -157.160nT. These values of the upward continuing field were less than the magnetic field of the crust (Figure 6).

Figure 6's upward continuing RTE map displays a similar distribution of strong and low magnetic anomalies. Anomalies on the upward continuing RTE map have values between around 279.141nT and 157.160nT. A prominent negative (long wavelength) anomaly is present on the upward continuing RTE map, which is essentially a smoothed version of the RTE map and is dispersed across the northeastern, central, and southern regions of our study area. The northern region of the image consistently displays prominent anomalies with long wavelength, low amplitude magnetic maxima and somewhat larger amplitude magnetic minima, which suggests that these anomalies are linked to deeper structures.

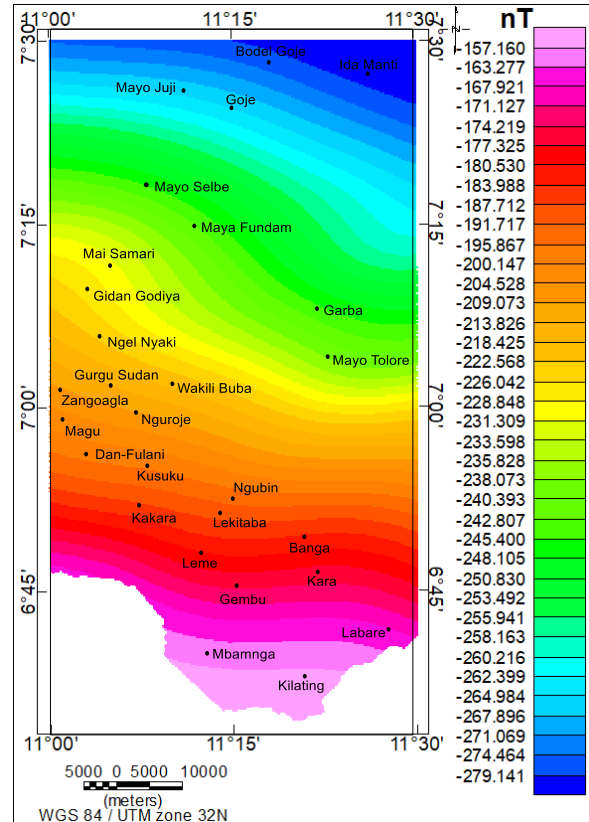


Figure 6: The Reduction Magnetic Equator map upward continued to 15 km of Mambilla and environs

Lineament Trend Analysis and Structural Density Map of the Area

The surficial lineaments, which indicate structural density zones, are automatically derived from satellite and aeromagnetic data (Figures 7 and 8). Because they are structurally controlled, the mining areas exhibit high structural density, highlighting the value of lineaments density maps in the identification of prospective mineralization zones (Abdelnasser and Kumral, 2017). As a result, a structural and lineament map using aeromagnetic, satellite, and data from Figure 7 were created. This map is based on lineament detection from these sources. The accompanying rise diagram from aeromagnetic and satellite data shows that it exhibits zones of high structural complexity characterised by a significant NE-SW trend along with less frequent NNW, WNW, NS, and NE tendencies (Figures 9 and 10). These developments and the trends in the zones of surface structural complexity of some well-known minerals show a favourable link. It includes illustrations of some of these mined solid minerals, such as blue sapphire, aquamarine, tourmaline, amethyst, cassiterite, and bauxite (e.g., Maisamari, Gurgu, Yelwa, Mayo Ndaga, Lekitaba, and Nguroje). to verify the effectiveness of the methods employed. There is a strong correlation between the primary trends that emerged from the current investigation and previous published field geoscientific data. According to Abdelnasser and Kumral (2017), mineralization occurs along brittle-ductile shear zones in the NE-SW direction at the Maisamari, Gurgu, Yelwa, Mayo Ndaga, Lekitaba, and Nguroje areas. Klemm and Klemm (2013) noted that the NW direction was a major trend for gold mineralization. El-Desoky et al. (2021) noted

that the structural elements (such as faults and shear zones) extending in NW-SE and N-S trends are connected with the gold mineralization. The majority of gold-quartz veins, according to Helmy et al. (2004), typically trend N-S, NNE-SSW, with the appearance of non-mineralized quartz veins flowing in the NW direction. Klemm and Klemm (2013) cited the principal mined quartz veins follow a shear zone of the NW and ENE-WSW directions, quartz lodes strike in the NE-SW direction. In order to establish the structural density zone, lineament density map (Figure 11) was additionally derived from the digital elevation model (Figure 12). According to Figure 11, which shows a positive link between higher lineament density and mineralization sites, the known present mining zones have areas with medium to high lineament densities.

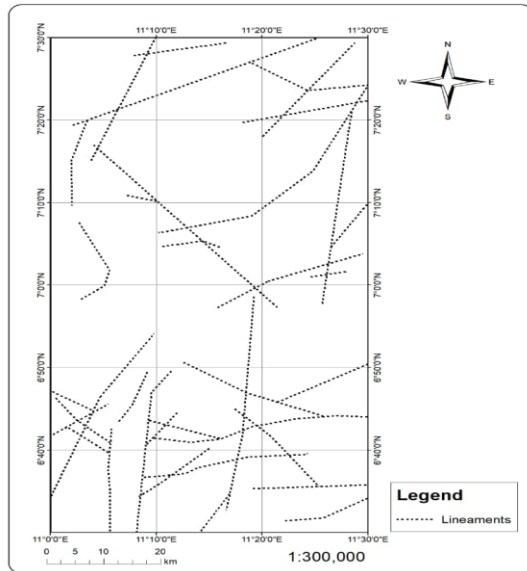


Figure 7: Structural lineaments map of the study area extracted from satellite data

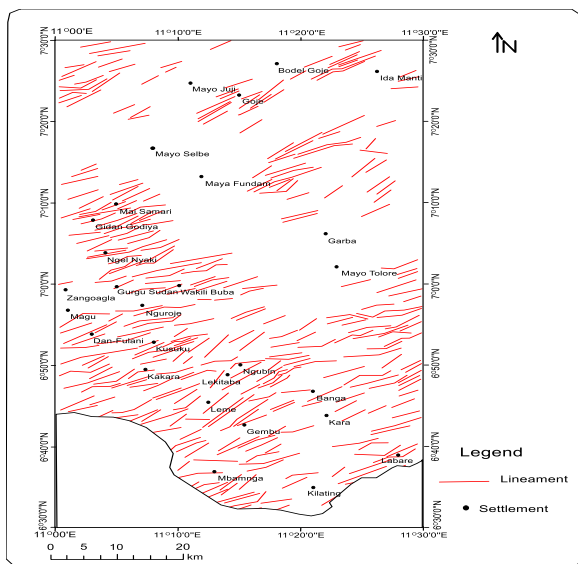


Figure 8: Structural lineaments map of the study area extracted from aeromagnetic data

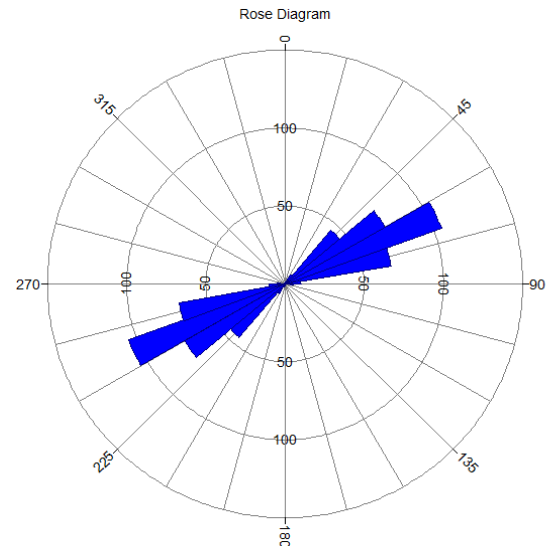


Figure 9: Rose diagram extracted from aeromagnetic data

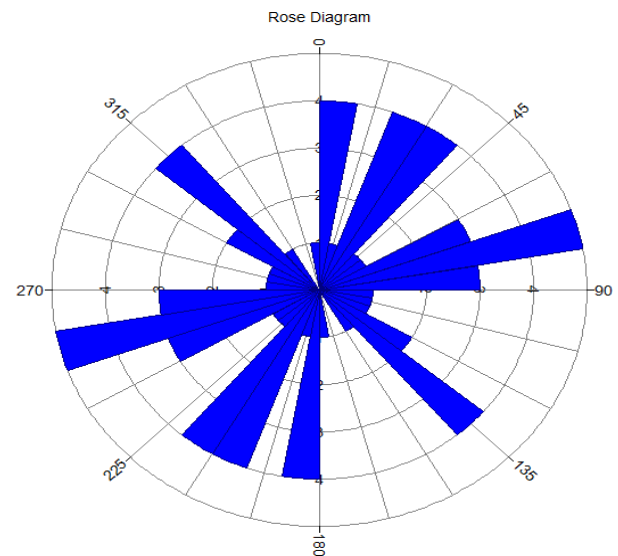


Figure 10: Rose diagram extracted from Satellite imagery

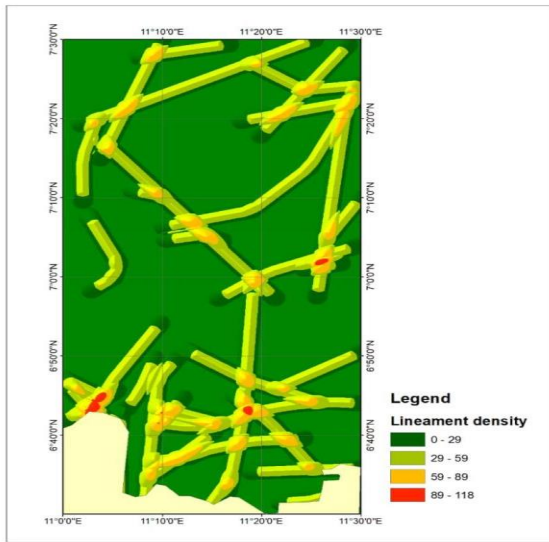


Figure 11: Lineament density map of the study area

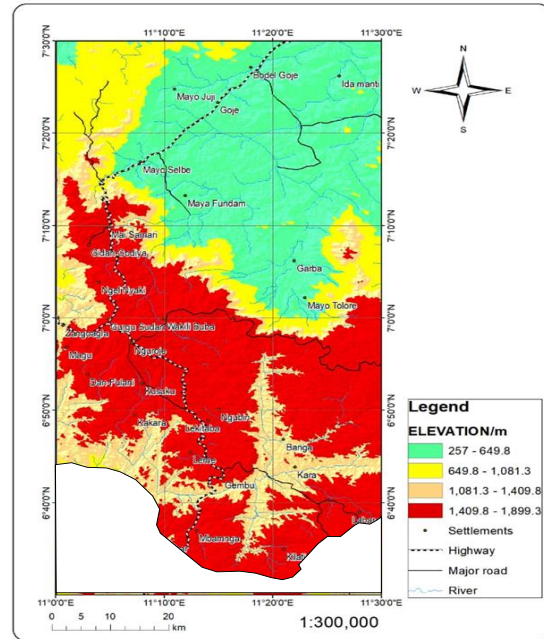


Figure 12: Digital elevation map of the study area

Magnetic Source Depths Determination over Mambilla and Environs

Using spectral analysis of 38 blocks, it was possible to calculate the depth to magnetic sources (Figure 13). The data in Table 2 show the shallow and deep magnetic sources in the region of the Gashaka sheet 275. The values from (Table 2 and 3) were used to create the maps in Figures 14 and 15. The results for the shallow source depth (D2) vary from 0.191 to 1.17 km with an average value of 0.461 km (Figure 15), and the values for the deeper source depth (D1) of Gashaka sheet 275 range from 0.593 to 4.42 km with an average value of 1.772 km (Table 2 and Figure 14). While the average magnetic depth of the deeper source (D1) of Mambilla sheet 275 spans from 0.354 to 4.76 km, with an average value of 1.241 km (Table 3) and the values for shallow source depth (D2) ranges from 0.062 to 0.608 km with an average value of 0.345 km.

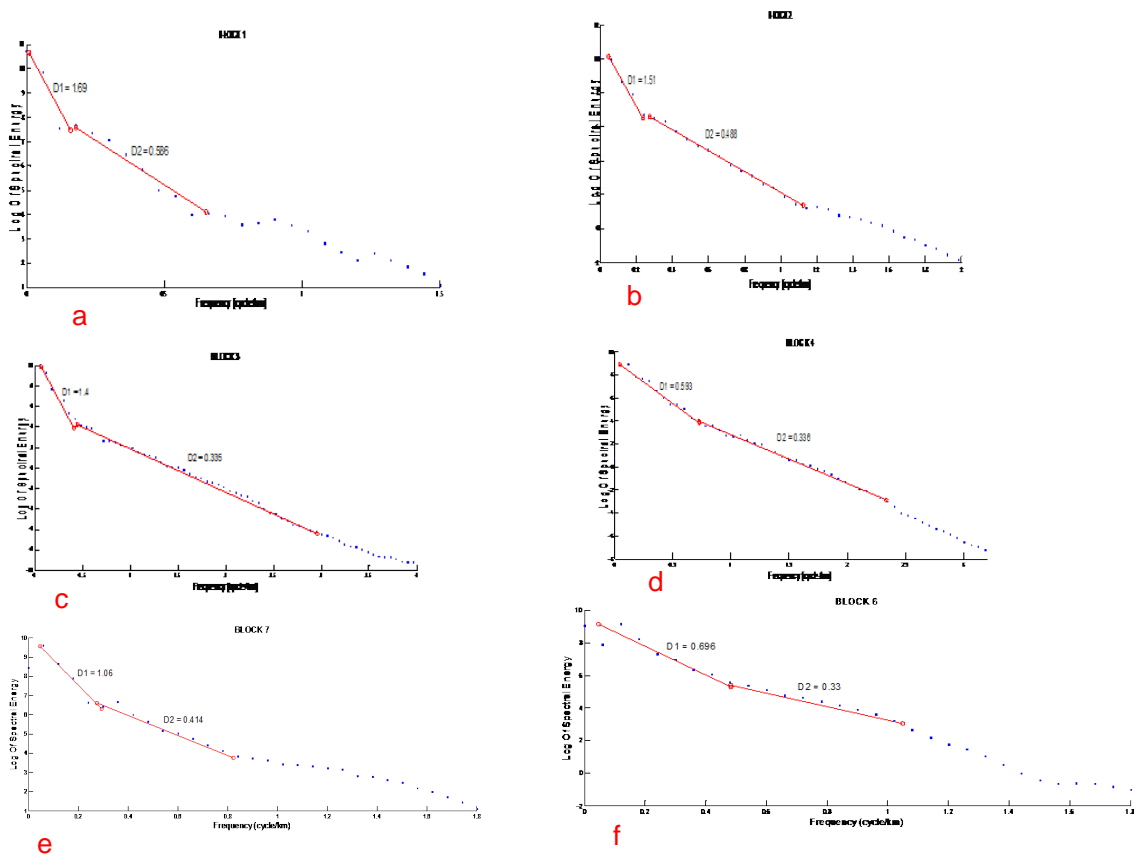


Figure. 14(a-f). Examples of spectral plot over Mambilla and environs

Table 2. Computed spectral analysis of the Mambilla sheet 295 of about 16 blocks in the study area.

Sheet Name	S/No	Spectral Block	Longitude		Latitude		Spectral Depth (km)	
			X1	X2	Y1	Y2	Deep source(D1)	Shallow source(D2)
	1	1	11.0	11.125	7.375	7.5	1.69	0.586
	2	2	11.125	11.25	7.375	7.5	1.51	0.488
	3	3	11.25	11.375	7.375	7.5	1.40	0.335
	4	4	11.375	11.5	7.375	7.5	0.593	0.336
	5	5	11.0	11.125	7.25	7.375	3.6	1.17
	6	6	11.125	11.25	7.25	7.375	0.696	0.33
	7	7	11.25	11.375	7.25	7.375	1.06	0.414
	8	8	11.375	11.5	7.25	7.375	2.19	0.477
	9	9	11.0	11.125	7.125	7.25	1.28	0.335
	10	10	11.125	11.25	7.125	7.25	0.869	0.191
	11	11	11.25	11.375	7.125	7.25	0.994	0.234
	12	12	11.375	11.5	7.125	7.25	1.78	0.554
	13	13	11.0	11.125	7.0	7.125	1.14	0.232
	14	14	11.125	11.25	7.0	7.125	4.42	0.529
	15	15	11.25	11.375	7.0	7.125	1.41	0.304
	16	16	11.375	11.5	7.0	7.125	3.72	0.856
Average							1.772	0.461

Table 3. Computed spectral analysis of the Gashaka sheet 276 of about 16 blocks in the study area.

Sheet Name	S/No	Spectral Block	Longitude		Latitude		Spectral Depth (km)	
			X1	X2	Y1	Y2	Deep source(D1)	Shallow source(D2)
Mambilla295	1	17	11.0	11.125	6.875	7.0	0.583	0.281
	2	18	11.125	11.25	6.875	7.0	0.56	0.179
	3	19	11.25	11.375	6.875	7.0	1.39	0.451
	4	20	11.375	11.5	6.875	7.0	1.39	0.422
	5	21	11.0	11.125	6.75	6.875	4.06	0.608
	6	22	11.125	11.25	6.75	6.875	1.91	0.537
	7	23	11.25	11.375	6.75	6.875	0.749	0.328
	8	24	11.375	11.5	6.75	6.875	2.29	0.323
	9	25	11.0	11.125	6.625	6.75	0.157	0.062
	10	26	11.125	11.25	6.625	6.75	0.551	0.28
	11	27	11.25	11.375	6.625	6.75	0.996	0.541
	12	28	11.375	11.5	6.625	6.75	1.79	0.546
	13	29	11.0	11.125	6.5	6.625	NA	NA
	14	30	11.125	11.25	6.5	6.625	0.903	0.278
	15	31	11.25	11.375	6.5	6.625	0.931	0.222
	16	32	11.375	11.5	6.5	6.625	0.354	0.11
Average							1.241	0.345

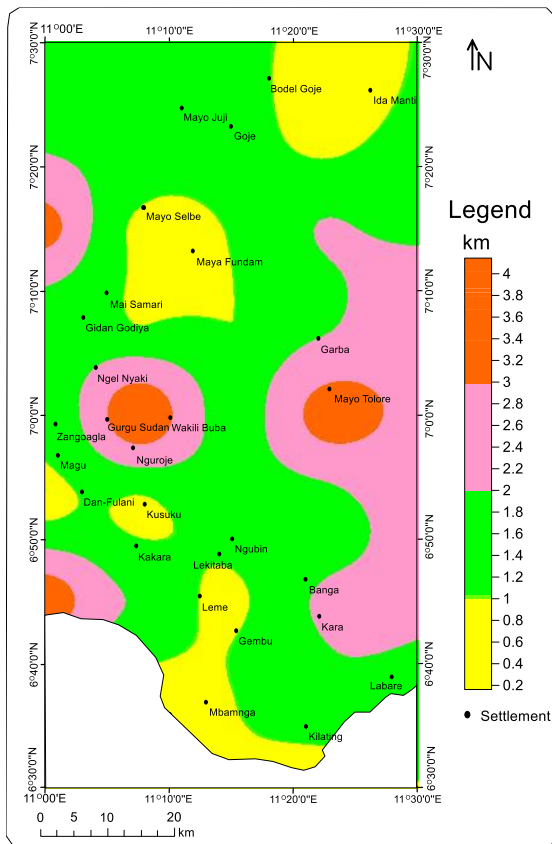


Figure 15: Magnetic Source to Deeper Sources over Mambilla and Environs

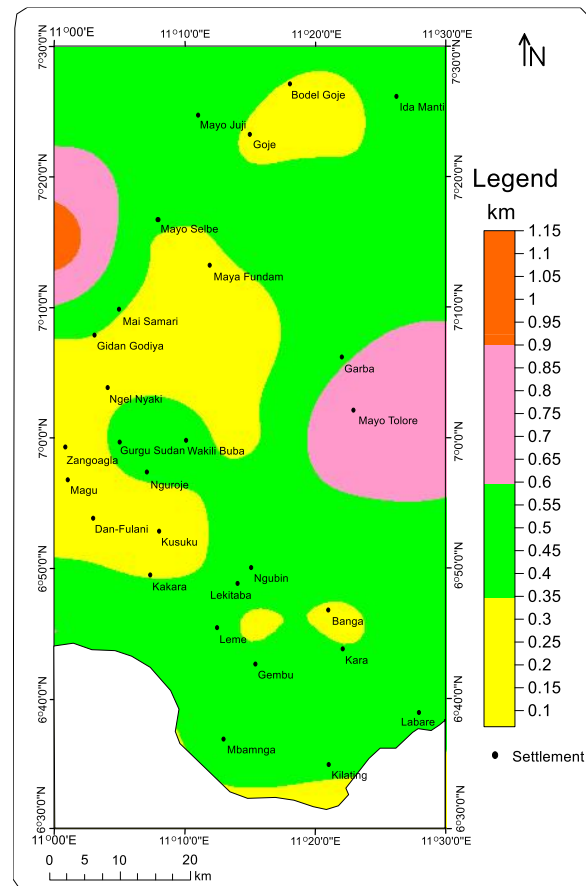


Figure 16: Magnetic Source to Shallow Sources over Mambilla and Environs

Curie Point Depth, Geothermal Gradient and Heat Flow over Mambilla and Environs

The area was divided into 32 blocks using spectral analysis. The Gashaka sheet 297 and the Mambilla sheet 295 both include sixteen blocks (Tables 2 and 3). It is well recognised that utilising a short window width when interpreting aeromagnetic data using spectral approaches can lead to errors Nwankwo and Shehu (2015). According to Mickus and Hussein (2015), the window size should be two to three times the depths to be calculated because it depends on how deep a magnetic susceptibility source is at the bottom. The upward continuing RTE data for each window was then computed to provide the 2D radial power spectrum (Figure 6). Next, a first-order polynomial trend surface for each block was used to remove the long wavelengths of regional magnetic anomalies, and the grids were expanded by 10% to lessen the edge effects of using the Fourier Transform in determining the power spectrum Khojamli et al (2016).

According to Mickus and Hussein (2015), the geology of a region affects the CPD. The entire region is characterised by shallow and deeper magnetic susceptibility sources (CPD), with depths to the bottom varying from 0.11 to 4.42 km. The shallow depths are between 0.11 and 1.17 kilometres, while the greater depths are between 0.56 and 4.42 kilometres. The findings mainly accorded with previously published works in the study area. Kasidi and Nur (2012) obtained 2km to 2.62km for deeper source and 70m to 0.63km for shallow source from curie depth isotherm deduced from spectral analysis of magnetic data over Sarti and Environs of North-Eastern Nigeria. Nur, Onuoha, and Ofoegbu (1999) obtained 1.6km to 5km for deeper source around middle Benue, while 60m to 1.2km was obtained for shallow magnetic source. The shallow depths found in this study may be the result of magmatic intrusions that may be connected to the CVL, whereas the other shallow depths are probably the result of rifting associated with the Benue Trough, according to Rankenburg et al. (2004). They might also be the locations of several thrust faults connected to the Pan African belt's collision tectonics, making them a region of thinner crust with higher heat flow values. Additionally, the nearby volcanic intrusion unit or the extension of the Chain fault in the study area may be to blame for the shallow Curie depth that was recorded. According to Arthaud et al. (1990), Piqué et al. (1999a, b), and Andrianaivo and Ramasiarino (2010), regions with shallow curie points are frequently found in extensional domains, where important features like faults and fractures serve as the geological controls on fluid flow. In these systems, free convection dominates the heat transfer mechanisms along the permeable fracture path, but heat conduction is more likely to happen outside of permeable fracture paths. Crustal thinning, which is regionally linked to recently crystallised intrusions and both of which heighten the geothermal gradient, is the primary cause of the heat. Because no probable units with primary porosity have been discovered, the deeper curie point depth may be connected to fractured Precambrian basement, which may represent the host rocks (Saibi et al., 2015; Melouah et al., 2021). Using Japan as an example, Tanaka, et al. (1999) demonstrated that CPDs are less than 10 km in volcanic and geothermal zones, between 15 and 25 km in island arcs, and more than 20 km in oceanic plateaus, but Mickus and Hussein (2015) found that CPDs in Precambrian terrains could be greater than 15 km.

the geothermal gradient and heat flow were inferred. From 3.54 km to 6.84 km are the estimated distances from the centroid. To the top of magnetic susceptibility sources, however, the depths varied from 0.55 km to 2.50 km. The bottom of the magnetic susceptibility sources, which was assumed to represent the CPD, can be found at depths ranging from 4.77 km to 12.23 km (Figure 17). The depths indicated by spectroscopy are consistent with those found by Kasidi and Nur (2012). The estimated depths to the upper boundary of the magnetic sources fell within a range that was well connected with other local investigations within and around the study area.

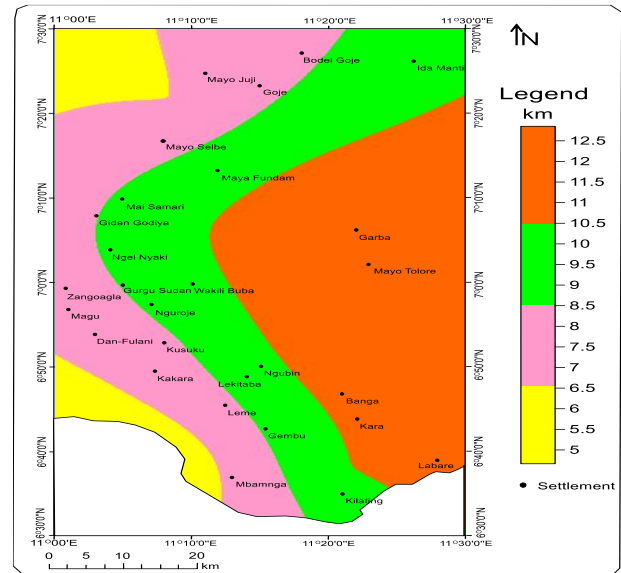


Figure 17: Curie point depth map of the Study area

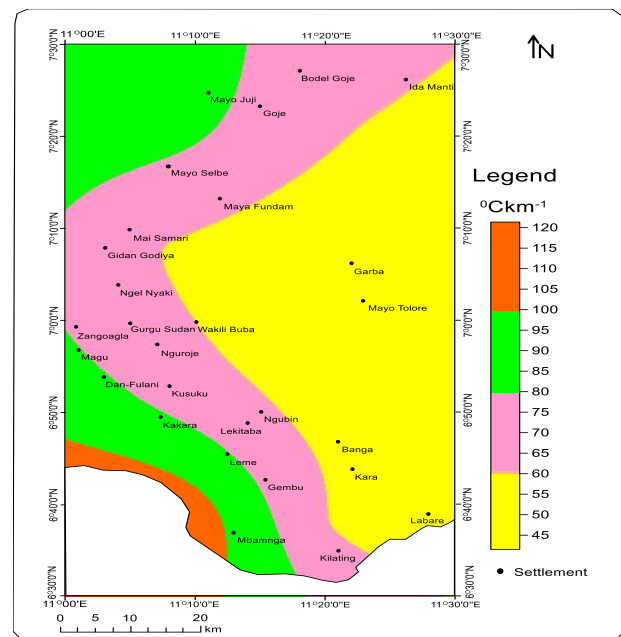


Figure 18: Geothermal Gradient Map of the Area

Table 4 displays the power spectrum analysis results, from which

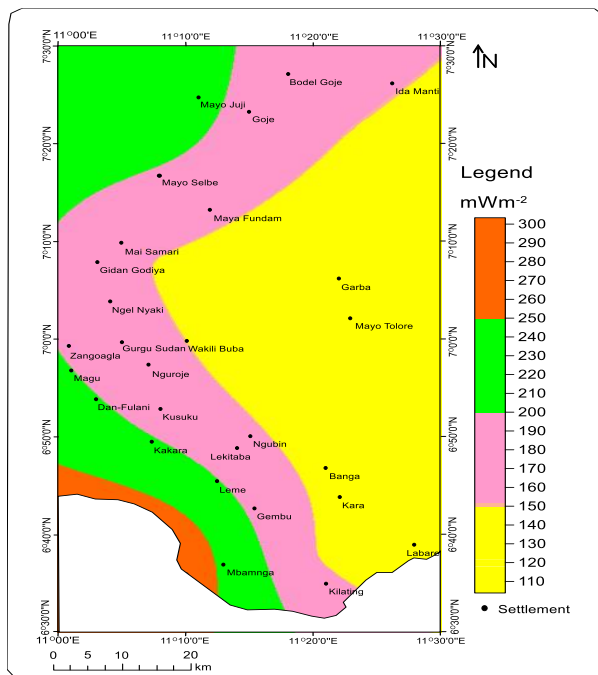


Figure 19: Heat Flow Map of the Study area

Table 4. Estimated CPD, geothermal gradients and heat flow over Mambilla and Environs.

S/No	Centroid Z_0 (km)	depth Z_1 (km)	Depth to top Z_t (km)	Depth to bottom Z_b (km)	Geothermal Gradient($^{\circ}\text{Ckm}^{-1}$)	Heat Flow (mWm^{-2})
1	3.64	0.86	6.42	90.33	225.82	
2	5.04	0.80	9.29	62.47	156.17	
3	5.53	1.14	9.92	58.47	146.17	
4	6.81	1.07	12.55	46.22	115.54	
5	4.57	1.02	8.12	71.43	178.57	
6	6.49	0.75	12.23	47.44	118.59	
7	2.66	0.55	4.77	121.62	304.05	
8	6.46	2.50	10.42	55.66	139.16	

CONCLUSION

By calculating the Curie point depth (CPD) and the geothermal gradient using aeromagnetic data, the viability of geothermal exploration was assessed. The isothermal surface at which magnetic materials lose their magnetism is defined by CPD as being at about 580°C . The residual magnetic map was created by processing the total magnetic intensity field and dividing it into overlapping blocks. Each block's spectral analysis was used to determine the depths to the top boundary (Z_t) and centroid (Z_0), and an empirical formula was used to determine the depths to the bottom of the magnetic sources and heat flow. The depth readings were then utilized to evaluate the area's geothermal gradient, heat flow, and curie point depths (CPD). Two CPD locations with geothermal potential are described in the results: areas with shallow curie point depths (0.11-1.72 km) and areas with deeper depths (0.34 - 4.46 km). The geothermal gradients measured range from 46.22 to $121.620^{\circ}\text{Ckm}^{-1}$, while the measured heat-flow values range from 139.16 to 304.05 mWm^{-2} .

The results obtained agreed with other published works in the study area. Nur et al (1999) obtained 1.6km to 5km for deeper source around middle Benue, while 60m to 1.2km was obtained for shallow magnetic source; Kasidi and Nur (2012) got 2km to 2.62km for

deeper source and 70m to 0.63km for shallow source from curie depth isotherm deduced from spectral analysis of magnetic data over Sarti and Environs of North-Eastern Nigeria. The shallow depths obtained from this study may be due to magmatic intrusions which could be related to the CVL, and the other shallow depths are likely due to the rifting related to the Benue Trough Rankenburg et al (2004). They may also be sites of numerous thrust faults related to the collision tectonics of the Pan African belt and thus may be a region of thinner crust with higher heat flow values. In addition, the shallow Curie depth observed could be a result of the volcanic intrusion unit spotted in the area or the extension of Chain fault in the study area. Regions with shallow curie point are commonly associated with extensional domains (Arthaud et al. 1990; Piqué et al. 1999a, b; Andrianaivo and Ramasiarino 2010a,b), where major structures such as faults and fractures are the geological controls on fluid flow. Such systems involve heat transfer mechanisms dominated by free convection along the permeable fracture path, whereas heat conduction is likely to occur outside permeable fracture paths. The main source of the heat is crustal thinning, which is locally associated with recently crystallized intrusions, both of which increase the geothermal gradient. The deeper curie point depth may be related to fractured

Precambrian basement, which may represent the host rocks (Saibi et al, 2015, Melouah et al, 2021). Tanaka, et al(1999) using Japan as an example showed that CPDs less than 10 km occur in volcanic and geothermal areas, between 15 - 25 km in island arcs, and deeper than 20 km in oceanic plateaus, while Mickus and Hussein (2015) showed that in Precambrian terrains these depths could be greater than 15 km.

This study also revealed strong and positive correlation with some African countries where geothermal energy are been utilized ((Githiri et al., 2012; Wheildon et al., 1994). Complex magmatic and tectonic linkages of large intrusions and fault systems, particularly the Chain faults that may have extended into the study area, which is responsible for the high geothermal energy and heat flow in the area. A common CPD of $3^{\circ}\text{C}100\text{m}^{-1}$ or $30^{\circ}\text{CKm}^{-1}$ and average thermal conductivity values ranging from 105.68 to 227.63mWm^{-2} are considered to have a good potential for geothermal energy. The potential for geothermal energy resources in the area is therefore very great. The study's most important and practical finding is that there is a good chance that the region will have geothermal energy resources, which may be used to power the government-owned Mambilla Hydro-Electric Power Plant as a reliable renewable energy source. As seen in the accompanying rose diagram from aeromagnetic and satellite data, the region exhibits zones of high structural complexity characterised by a significant NE-SW trend along with less frequent NNW, WNW, NS, and NE trends.

ACKNOWLEDGEMENT

The high-resolution aeromagnetic data for this research was bought from the Nigerian Geological Survey Agency (NGSA), Abuja. I would like to offer my sincere gratitude to the entire staff of the Nigerian Geological Survey Agency (NGSA), Abuja, for running an open door policies to researchers.

REFERENCES

- Abdel Zaher M, Elbarbary S, El-Shahat A, Mesbah H, Embaby A(2018). Geothermal resources in Egypt integrated with GIS-based analysis. *J VolcanolGeotherm Res.*;365:1–12.
- Abdelnasser, A., Kumral, M., (2017).The nature of gold-bearing fluids in Atud gold deposit, Central Eastern Desert, Egypt. *Int. Geol. Rev.* 59 (15), 1845–1860. <https://doi.org/10.1080/00206814.2017.1299043>
- Abaa, S.I. and Najime, T. (2006). Mineralization in Precambrian rocks of central Nigeria: Implications for the Oban – Budu – Mandara – Gwoza complex of eastern Nigeria. *Global Journal of Geological Sciences*, 4 (2): 121 – 128.
- Ait OA, Issaadi A, Maizi D, Ayadi A, Bouhdjar A(2019). Geothermal potential in the Ouarsenis-Biban-Kabylie (North Central Algeria):hot spring catalogue. *Arab J Geosci.*12:741.
- Ajibade C. A., Woakes M., Rahaman M. A., (1989). Proterozoic Crustal Development in the Pan-African Regime of Nigeria. In: Kogbe C. A. (ed.) *Geology of Nigeria*. 2nd Revised Edition, Abiprint&PakLtd.,Ibadan.
- Andrianaivo L, RamasiarinoV(2010a). Structural model of the Itasy geothermal prospect in central Madagascar: preliminary review. In: World geothermal congress; 25–29 April Bali, Indonesia. 2010a.
- Andrianaivo L, Ramasiarino V.J.(2010b) Relation between regional lineament systems and geological structures: implications for understanding structural controls of geothermal system in the volcanic area of Itasy, Central Madagascar. In: World geothermal congress 2010; 25–29 April, Bali, Indonesia.
- Anudu GK, Stephenson RA, Macdonald DIM. Using high-resolution aeromagnetic data to recognize and map intra-sedimentary volcanic rocks and geological structures across the Cretaceous middle Benue Trough, Nigeria. *J Afr Earth Sci.* 2014;99:625–36.
- Arthaud F, Grillot J-C, Raunet M. (1990). Tectonique cassante à Madagascar: son incidence sur la géomorphologie et sur les écoulements. *Can J Earth Sci.* 27:1394–407.
- Awoyemi MO, Hamed OS, Falade SC, Arogundade AB, Ajama OD, Iwalehin PO, et al. Geophysical investigation of the possible extension of Ifewara fault zone beyond Ilesa area, southwestern Nigeria. *Arab J Geosci.* 2017;10(27):1–14.
- Awoyemi MO, Arogundade AB, Falade SC, Ariyibi EA, Hamed OS, Alao OA, et al. Investigation of basement fault propagation in Chad Basin of Nigeria using high resolution aeromagnetic data. *Arab J Geosci.* 2016;9(453):1–20
- Awoyemi MO, Ajama OD, Hamed OS, Arogundade AB, Falade SC. Geophysical mapping of buried faults in parts of Bida Basin, North Central Nigeria. *Geophys Prospecting.* 2018;66:40–54.
- Bansal, A.R., Gabriel, G., Dimri, V.P. and Krawczyk, C.M. (2011) Estimation of Depth to the Bottom of Magnetic Sources by a Modified Centroid Method for Fractal Distribution of Sources: An Application to Aeromagnetic Data in Germany. *Geophysics*, 76, L11-L22.
- BekeleB(2012). Review and reinterpretation of geophysical data of tendaho geothermal field. Addis Ababa: Geological Survey of Ethiopia 2.
- Benkhelil J., (1988). Structure et evolution geodynamique du basin intracontinental de la Benoue (Nigeria). *Bulletin CentresRecherchers Exploration-Production Elf-Aquitaine* 12, pp 29-128.
- Benkhelil J., Guiraud M., Ponsard J. F., Saugy L., (1989). The Bornu-Benue Trough, The Niger Delta and its Offshore: Tectono-Sedimentary reconstruction during the Cretaceous and Tertiary from geophysical data and Geology. In: Kogbe C. A. (ed.) *Geology of Nigeria*. 2nd Revised Edition, Abiprint&Pak Ltd., Ibadan.
- Bhattacharyya, B.K., Leu, L.K., 1975. Analysis of magnetic anomalies over Yellowstone National Park: mapping the Curie point depth isothermal surface for geothermal reconnaissance. *J. Geophys. Res.* 80, 4461e4465. <http://dx.doi.org/10.1029/JB080i032p04461>.
- Blackwell, D.D. (1971) *The Thermal Structure of the Continental Crust. The Structure and Physical Properties of the Earth's Crust*, Geophysical Monograph Series, 14, 169-184.
- Blakely, R.J., 1995. *Potential Theory in Gravity and Magnetic Applications*. Cambridge University Press, London
- Black R (1980) Precambrian Geology of West Africa. *Episodes* 4:3–8
- Burke KC, Dewey JF (1972) Orogeny in Africa. In: Dessauvage TFJ, Whiteman AJ (eds), *Africa geology*. University of Ibadan Press, Ibadan, pp 583–608
- Cermak, V. and Rybach, L. (1982) *Thermal Conductivity and*

- Specific Heat of Minerals and Rocks. Springer-Verlag Publishing, Berlin
- Dada .S.S (2006). Proterozoic evolution of Nigeria. In: Oshi O (ed) The basement complex of Nigeria and its mineral resources (A Tribute to Prof. M. A. O. Rahaman). Akin Jinad& Co. Ibadan, pp 29–40
- De Ritis, R., Ravat, D., Ventura, G., Chiappini, M., 2013. Curie isotherm depth from aeromagnetic data constraining shallow heat source depths in the central aeolian ridge (southern Tyrrhenian Sea, Italy). *Bull. Volcanol.* 75 (710), 11. <http://dx.doi.org/10.1007/s00445-013-0710-9>.
- Dickson MH, Fanelh M. What is geothermal energy? [online]. <http://www.geothermalenergy.org/geo/geoenergy.php>; 2004.
- Dhansay T, Wit M, PattA(2014). An evaluation for harnessing low-enthalpy geothermal energy in the Limpopo Province, South Africa. *S Afr J Sci.* 110:1–10.
- Dupreez.J.W, Barber W (1965).The distribution and chemical quality of ground water in Northern Nigeria.*Bulletin* 36.*Geological survey of Nigeria* 93.
- EIA, 2007. Environment Impact Assessment (EIA) 2007.
- Elbarbary S, Zaher MA, Mesbah H, El-Shahat A, EmbabyA(2018). Curie point depth, heat flow and geothermal gradient maps of Egypt deduced from aeromagnetic data. *Renew Sustain Energy Rev*;91:620–9.
- El-Desoky, H.M., Shahin, T.M., Amer, Y.Z., 2021. Characteristic of gold mineralization associated with granites at Hamash old gold mine, South Eastern Desert, Egypt. *Arab. J. Geosci.* 14 (7).
- Enerdata(2013). Global Energy Statistical Yearbook, Enerdata, Grenoble, France.
- Eyike, A., Werner, S.C., Ebbing, J. and Dicoum, E.M. (2010) On the Use of Global Potential Field Models for Regional Interpretation of the West and Central African Rift System. *Tectonophysics*, 492, 25-39.
- Frantz C (1981). Development without communities: Social fields, Network and Action in the Mambilla Grasslands of Nigeria. *J. Human org.* pp. 211-220
- GEA. Geothermal electric production potential, based upon US Geologic Survey Testimony before the Subcommittee on Energy and Mineral Resources of the House Resources Committee [online]. <http://www.geo-energy.org/UsResources.htm>; 2001.
- Githiri J.G, Patel J.P, Barongo J.O, Karanja P.K(2012). Spectral analysis of ground magnetic data in Magadi area, Southern Kenya Rift. *Tanz J Sci.* 2012;38:1–14.
- Grant N. K., Rex D. C., Freeth S. J., 1972. Potassium- Argon Ages and Strontium Isotope Ratio Measurements from Volcanic Rocks in Northern Nigeria. *Contr. Mineral and Petrol.* 35, 277- 292.
- Hafner M, Tagliapietra S, de StrasserL(2018). Prospects for Renewable Energy in Africa. In: *Energy in Africa*, SpringerBriefs in Energy. Cham: Springer. pp. 47–75.
- Helaly, S.A. (2019) Imaging the Curie Point Isothermal Surface and Predicting Its Impact on the Geothermal Regime within the Nile Delta, Egypt. *Egyptian Journal of Petroleum*, 28, 77-90.
- Hodgson N, Rodriguez K, Intawonga(2017). The Angle of the North - Shallow water oil is hidden in plain sight in North Gabon. *GEO ExPro*;14(2):52–53.
- Jessop, A., Hobart, M. and Sclater, J. (1976) The World Heat Flow Data Collection 1975, Geothermal Services of Canada. Geothermal Service, 50, 55-77.
- Jeje LK (1983). Aspects of geomorphology of Nigeria. Heinemann educational books.
- Kappelmeyer O, Haenl R (1974) *Geothermics*. Borntraeger, Berlin, 238 pp
- Kasidi, S. and Nur, A. (2012) Curie Depth Isotherm Deduced from Spectral Analysis of Magnetic Data over Sarti and Environs of North-Eastern Nigeria. *School Journal of Biotechnology*, 1, 49-56.
- Khojamli, A., Ardejani, F., Moradzadeh, A., Kalate, A., Kahoo, A. and Porkhial, S. (2016) Estimation of Curie Point Depths and Heat Flow from Ardebil Province, Iran, Using Aeromagnetic Data. *Arabian Journal of Geosciences*, 9, 383-393.
- Klemm, R., Klemm, D., 2013. Gold and gold mining in ancient Egypt and Nubia. Springer. <https://doi.org/10.1007/978-3-642-22508-6>.
- Kogbe C. A., 1979. Geology of the South Eastern (Sokoto) Sector of the lullemeden Basin. *Bull. Dept. Geol., ABU, Zaria, Nigeria*, Vol. 2, No. 1.
- Kurowska, E and Schoeneich, K.(2010). Geothermal Exploration in Nigeria. *Proceedings World Geothermal Congress 2010*, Bali, Indonesia, 25-29 April 2010.
- Lachenbruch AH (1970) Crustal temperature and heat production: implications of the linear heat flow relation. *J Geophys Res* 75:3291–3330.
- Leseane K, Atekwana EA, Mickus KL, Abdelsalam MG, Shemang EM, Atekwana EA(2015). Thermal perturbations beneath the incipient Okavango Rift Zone, northwest Botswana. *J Geophys Res Solid Earth*;120:1210–28.
- Lee W.H.K, Uyeda S (1965) Review of heat-flow data. W.H.K. Lee, *Terrestrial Heat-Flow. Geophys. Monogr. Am. Geophys. Union*, pp 87–190. ISBN 8
- Likkason, O. K, Singh, G .P, and N. K. Samaila, N .K (2013). A Study of the Middle Benue Trough (Nigeria) Based on Geological Application and Analyses of Spectra of Aeromagnetic Data. *Energy Sources, Part A*, 35:706–716. Copyright © Taylor & Francis Group, LLC ISSN: 1556-7036 print/1556-7230 online DOI: 10.1080/15567036.2010.514588.
- Mattick R. E., 1982. Assessment of the petroleum, coal, and geothermal resources of the Economic Community of West African States (ECOWAS) region. United States Department of the Interior Geological Survey.
- Maden, N., (2010). Curie-point depth from spectral analysis of magnetic data in Erciyes stratovolcano (central Turkey). *Pure Appl. Geophys.* 167 (3), 349-358.
- Meliani O, Bourmatte A, Hamoudi M, Haddoum H, Quesnel Y(2016). Moho depth derived from gravity and magnetic data in the Southern Atlas Flexure (Algeria). *J Afr Earth Sci*;121:100–7.
- Melouah, O, Eldosouky, A.M and Ebong, E.D. (2021). Crustal architecture, heat transfer modes and geothermal energy potentials of the Algerian Triassic provinces. *Geothermics xxx (xxxx) 102211*

- Mickus, K. and Hussein, M. (2015) Curie Depth Analysis of the Salton Sea Region, Southern California Pure and Applied Geophysics, 172, 1383-1780.
- Montaj Oasis. Standard edition version 6.4.2 (HJ), Help: Help Topics. GeosoftInc; (2007).
- Mono, J.A., Ndougsa-Mbarga, T., Tarek, Y., Ngho, J.D. and OwonoAmougou, O.U.I. (2018). Estimation of Curie-Point Depths, Geothermal Gradients and Near-Surface Heat Flow from Spectral Analysis of Aeromagnetic Data in the Loum-Minta Area (Centre-East Cameroon). Egyptian Journal of Petroleum, 27, 1291-1299.
- Mubi AM, Tukur. A.L (2005). Geology and relief of Nigeria. Nigeria. Heinemann educational books.
- Ngho, J.D., NdougsaMbarga, T., Assembe, S.P., Meying, A., OwonoAmougou, O.U.I. and Tabod, C.T. (2017). Evidence of Structural Facts Inferred from Aeromagnetic Data Analysis over the Guider-Maroua Area (Northern Cameroon). International Journal of Geosciences, 8, 781-800.
- Ngako, V., Affaton, P. and Njonfang, E. (2008) Pan-African Tectonics in Northwestern Cameroon Implication for the History of Western Gondwana. Gondwana Research, 14, 509-522.
- Nigerian Geological Survey Agency (NGSA). Airborne geophysical survey total magnetic intensity map of Lagos–Ore axis, 2008.
- Noutchogwe, C., Tabod, C., & Manguelle-Dicoum, E. (2006). A gravity study of the Crustal beneath the Adamawa Fault Zone, West Central Africa. *Journal of Geophysics and Engineering*, 3, 82-89. <https://doi.org/10.1088/1742-2132/3/1/009>
- Nur, A., Ofoegbu, C.O. and Onuoha, K.M. (1999). Estimation of depth to the Curie point isotherm in the Upper Benue Trough, Nigeria. *Jour. Mining and Geol.* 35(1): 53 – 60.
- Nwankwo, L. and Shehu, A. (2015). Evaluation of Curie-Point Depths, Geothermal Gradients and Near-Surface Heat Flow from High-Resolution Aeromagnetic (HRAM) Data of the Entire Sokoto Basin, Nigeria. *Journal of Volcanology and Geothermal Research*, 305, 45-55.
- Obaje N.G. (2009). The Basement Complex. In: *Geology and Mineral Resources of Nigeria. Lecture Notes in Earth Sciences*, vol 120. Springer, Berlin, Heidelberg.
- Ogunmola JK, Ayolabi EA, Olobaniyi SB. Structural-depth analysis of the Yola arm of the Upper Benue Trough of Nigeria using high resolution aeromagnetic data. *J Afr Earth Sci.* 2016;124:32–43.
- Ojo S. B., Ajakaiye D. E., (1989). Preliminary interpretation of Gravity Measurements in the Middle Niger Basin Area, Nigeria. In: Kogbe C. A. (ed.) *Geology of Nigeria*. 2nd Revised Edition, Abiprint&Pak Ltd., Ibadan.
- Okubo, Y., Graf, R.J., Hansen, R.O., Ogowa, K., Tsu, H., 1985. Curie point depth of the island of Kyushu and surrounding areas, Japan. *Geophysics* 50, 481- 494.
- Okpoli C.C. High resolution magnetic field signatures over Akure and its Environs, southwestern Nigeria. *Earth Sci Malays.* 2019;3(1):9–17.
- Oladunjoye MA, Olayinka Al, Alaba M, Adabanja MA. Interpretation of high resolution aeromagnetic data for lineaments study and occurrence of banded Iron formation in Ogbomoso area, southwestern Nigeria. *J Afr Earth Sci.* 2016;114:43–53.
- Olasunkanmi NK, Bamigboye OS, Aina A. Exploration for iron ore in Agbado-OkuduKogi state, Nigeria. *Arab J Geosci.* 2017;10:541.
- Olasunkanmi NK, Sunmonu LA, Adabanija MA, Oladejo OP. Interpretation of high resolution aeromagnetic data for mineral prospect in Igbeti-Moro area, southwestern Nigeria. *IOP Conf Ser Earth Environ Sci.* 2018;173:012033.
- Ostaficzuk S., 1996. Geo-ecology of the Nigerian Part of the Lake Chad Basin. University of Silesia Press, Katowice.
- Omokpariola, C.E and Anakwuba, K.E (2022). Delineation of Geothermal Energy Potentials in Parts of Calabar Flank, Southeastern Nigeria Using Aeromagnetic Data. *WSN* 164 (2022) 77-107.
- Patterson NR, Reeves CV. Effects of the equatorial electrojet on aeromagnetic data acquisition. *J Int Geophys.* 1985;65(2):55.
- Piqué A, Laville E, Bignot G, Rabarimanana M, Thouin C. The initiation and development of the Morondava Basin [Madagascar] from the late carboniferous to the Middle Jurassic: sedimentary, palaeontological and structural data. *J Afr Earth Sci.* 1999a;28:931–48.
- Piqué A, Laville E, Chotin P, Chorowicz J, Rakotondraompiana S, Thouin C. L'extension à Madagascar du Néogène à l'Actuel: arguments structuraux et géophysiques. *J Afr Earth Sci.* 1999b;28:975–83.
- Pollack HN, Hurter SJ, Johnson JR (1993) Heat flow from the earth's interior: analysis of global data set: *Reviews of Geophysics* 31:267–280
- Rankenburg, K., Lassiter, J.C. and Brey, G. (2004) Origin of Megacrysts in Volcanic Rocks of the Cameroon Volcanic Chain—Constraints on Magma Genesis and Crustal Contamination. *Contributions to Mineralogy and Petrology*, 147, 129-144.
- Saibi A, Ehara S, Fujimitsu Y, Nishijima J (2006). Progress of geothermal development in Algeria. *J Volcanol Geotherm Res Jpn*;28(4):383–97.
- Saibi, H, Aboud, E. and Azizi, M., (2015). Curie point depth map for Western Afghanistan deduced from the analysis of aeromagnetic data, *Proceedings World Geothermal Congress 2015, Melbourne, Australia*, pp.19-25.
- Saleh S, Salk M, Pamukcu O (2013). Estimating Curie point depth and heat flow map for northern Red Sea rift of Egypt and its surroundings, from aeromagnetic data. *Pure Appl Geophys*;170:863–85.
- Sass J.H and Behrendt J.C (1980). Heat flow from the Liberian Precambrian shield. *J Geophys Res Solid Earth*;85:3159–62.
- Samah E, Mohamed A, Hakim S, Abdel R. F and Kamal S (2022). Geothermal renewable energy prospects of the African continent using GIS. National Research Institute of Astronomy and Geophysics (NRIAG), Helwan, Cairo 11421
- Schito A, Corrado S, Aldega L, Grigo D (2016). Overcoming pitfalls of vitrinite reflectance measurements in the assessment of thermal maturity: the case history of the lower Congo basin. *Mar Pet Geol*;74:59–70.
- Shibaki M, Beck F. Geothermal energy for electric power—a REPP Issue Brief [online]. http://www.repp.org/articles/static/1/binaries/Geothermal_Issue_Brief.pdf; 2003.

- Sinzinkayo JM, Sliwa T, WakanaF(2015). Directions of Energy Balance Improvement in Burundi in the Aspect of Geothermal Energy Resources. Proc. World Geothermal Congress (2015), Melbourne, Australia, 19–25.
- Stampolidis, A., Kane, I., Tsokas, G.N., Tsourlos, P., 2005. Curie point depths of Albania inferred from ground total field magnetic data. *Surv.Geophys.* 26 (4), 461- 480.
- Shuey, R.T., Schellinger, D.K., Tripp, A.C., Alley, L.B., 1977. Curie depth determination from aeromagnetic spectra, *geophys. J. Roy. Astr. Soc.* 50, 75-101.
- Tanaka, a., okubo, y., matsubayashi, O., (1999). Curie point depth based on spectrum Analysis of the magnetic anomaly data in east and southeast asia. *Tectonophysics* 306, 461-470.
- TeklemariamZ(2018). Geothermal outlook in East Africa and contribution of UNU-GTP in capacity building, UNU-GTP 40th Anniversary Workshop, Reykjavik, Iceland, 10.
- Turcotte, D.L., Schubert, G., 1982. *Geodynamics*. Cambridge University Press, New York.
- Tukur, A. L, Adebayo. A. A, Galtima A (2005). *The land and people of the Mambilla Plateau, Nigeria*. Heinemann educational books.
- Turner D. C., 1978. Volcanoes of the Biu Basalt Plateau, Northeastern Nigeria. *J. Mining and Geology*, Vol. 15, No. 2, 49-63.
- USD/EO/EERE.U.S. Department of Energy Office of Energy Efficiency and Renewable Energy [online]. http://www.eren.doe.gov/state_energy/technologyoverview.cfm?techid=5, 2002.
- Verheijen P.J.T and Ajakaiye D.E (1979). Heat-flow measurements in the Ririwai ring complex, Nigeria. *Tectonophysics* 54:T27–T32
- WaringG.A(1983). Thermal springs of the united states and other countries of the world—a summary. Geological Survey professional Paper 492. United States Department of the Interior.USGS.
- Wheildon J, Morgan P, Williamson K.H, Evans T.R, Swanberg C.A(1994). Heat flow in the Kenya rift zone. *Tectonophysics*,236:131–49.
- Yohanna .A, Likkason.O.K, Maigari A. S, Ali . S, Iyakwari .S, Adamu A, Frankie O.B, Musa. N, Rawen B. O and Ombugu G.(2023). Curie point Depth Estimation for Geothermal Reconnaissance Deduced from Aeromagnetic Data over the Mambilla Plateau and Environs, Northeastern Nigeria.Unpublished article.